# PHYSISORPTION OF WATER ON $SiO_2$–$TiO_2$–$Al_2O_3$ FILMS STUDIED BY IMPEDANCE SPECTROSCOPY

#ALFONZ PLŠKO*, KATARÍNA FATURÍKOVÁ**, JANA PAGÁČOVÁ***, MAREK LIŠKA****

* *Alexander Dubček University of Trenčín, Študentská 2, Trenčín SK-911 50, Slovakia*
** *Institute of Inorganic Chemistry, Slovak Academy of Sciences, Dubravská cesta 9, Bratislava SK-845 36, Slovakia*
*** *Faculty of Industrial Technologies, Alexander Dubček University of Trenčín, I. Krasku 491/34, Púchov SK-020 01, Slovakia*
**** *Vitrum Laugaricio – Joint Glass Center of the Institute of Inorganic Chemistry, Slovak Academy of Sciences; Alexander Dubček University of Trenčín; Faculty of Chemical and Food Technology, Slovak Technical University and Rona Inc.; Alexander Dubček University of Trenčín, Študentská 2, Trenčín SK-911 50, Slovakia*

#E-mail: alfonz.plsko@tnuni.sk

Submitted September 27, 2014; accepted June 26, 2015

**Keywords:** Sol-gel, Films, Physisorption of water, Impedance spectroscopy

*The influence of film composition and surface roughness on process of physisorption of water on $SiO_2$–$TiO_2$–$Al_2O_3$ films prepared by sol-gel method was studied by impedance spectroscopy. The composition of prepared films, expressed by $SiO_2$:$TiO_2$:$Al_2O_3$ ratio, was in the range of following molar ratio: 0:0.95:0.05; 0.32:0.63:0.05; 0.475:0.475:0.05; 0.63:0.32:0.05; 0.95:0:0.05. Complex impedance spectra of thin film sensor for various relative humidities were measured in the range of 0.13 - 97.7 % and the frequency range was 1 kHz to 1 MHz. Measured dependences of complex impedance on frequency were processed by complex nonlinear least squares method. Serial connection with different counts of -(R/C)-, -(R/CPE)- and -R- equivalent circuits was used to analyse obtained spectra. The equivalent circuits were associated with physisorption of water, space charge polarization regions, and bulk or surface conductivity of the films. The dependencies presence of the relaxation processes on the value of relative humidity is used to analyse the process of water physisorption and determine composition influence, too.*

## INTRODUCTION

Humidity sensors based on metal oxides have wide range of application. Main advantages of these are high lifetime and temperature stability. Materials based on metal oxides, used either as bulk or as films, are characterized by indicated change of material properties where the given change is induced by adsorption of air humidity [1, 2]. This type of material surface adsorption is called physical adsorption and it is reversible [3-5]. The creation of adsorbed water layer on the material surface is function of concentration of water in the surroundings of sensor and surface concentration of –OH groups which depends on the type of material used as the sensitive layer of sensor [6, 7]. These –OH groups act as reaction centres on which water molecules are attached by hydrogen bonds. Water molecule is bonded on two adjacent –OH groups in the first step of adsorption. The interaction of external field causes that the molecules of water bonded in this way are consequently reoriented in a more difficult way. As adsorption is in progress, the islets of adsorbed water grow and subsequently, these islets create a monomolecular layer of adsorbed water. When the humidity is high, more layers of physisorpted water are created. Water molecules in these layers are usually bonded by one hydrogen bond to the previous layer and by another bond to the water molecule in the same or higher layer. Mobility of physically bounded water molecules in these layers is higher and also their reorientation caused by the influence of external field is not so complicated. When the way of water bonding in adsorbed layer is changed, it leads to changes in mobility of water molecules and it means the change in dielectric properties and conductivity of materials with adsorbed water layer [8-11]. Hydroxyl groups on the material surface are created by chemical reaction between surface and humidity from surroundings. In this reaction the M–O–M (M stands for metal) bond is cleaved and two M–OH groups are formed. This chemical reaction occurs on the surface of oxidic materials during their cooling after the thermal treatment. At room temperature, the reaction is considered as irreversible. This process is called chemisorption [3, 4].

Sol-gel method is based on controlled hydrolysis of oxide precursors where M–OH groups are created, and M–OH or M–OR groups are subsequently chain in condensation reactions where M–O–M bond as well as $H_2O$ or ROH molecule are created. Condensation reactions lead to creation of oxide oligomers which are connected to space units by condensation reactions and

following formation of particles. When these particles reach the diameter from 5 to 50 nm (according to the type of oxide), they form sols. Particles of sol include M–O–M bonds characteristic for bulk oxides, as well as many M–OH groups. Mostly they are localized on the particle surface. Sols are metastable colloidal systems and they precipitate or form gels by condensation between M–OH groups of two different particles. After the gel's formation, the densification occurs due to removal of disperse medium. When the most part of disperse medium is removed, inorganic gels form xerogels. Original structure of xerogel cannot be renewed by addition of disperse medium. The densification of xerogels occurs at higher temperature and is connected with continuation condensation reactions between M–OH groups which are in xerogel's structure. The final product is considered as oxide or oxides with the residual –OH groups. One of the advantages of sol-gel method is that it can be used for preparation of sols with particles which consist of several oxides and they are homogeneous on the molecular level [12-14]. However, during the cooling of such product, the water on the material surface is chemisorbed and M–OH groups are formed [7, 10]. These groups then acts as reaction centres for physical adsorption of water on the surface.

When films are prepared by sol-gel method, sols of defined composition are deposited on the substrate. Process of gelation and drying leading to creation of xerogel takes place in the surface film and it is very fast. Thermal treatment, which provides densification of prepared film, is done mainly in the temperature interval from 150 to 500°C. Properties of substrate and requirements for prepared film (porosity, concentration of residual M–OH groups and degree of water chemisorption during cooling of film from thermal treatment temperature to room temperature) are limiting factors. Films prepared by sol-gel method have wide range of applications in optics, protection of materials and humidity sensors [15, 16]. The films of $BaTiO_3$ [17], $Al_2O_3$ [18], $TiO_2$ [19], $SiO_2$–$TiO_2$–$Al_2O_3$ [20, 21] and $TiO_2$–$ZrO_2$ [22] were investigated as humidity sensors. The impedance spectroscopy is used for study of dielectric properties of films prepared by sol-gel method [23-26].

A detailed physico-electrical model of all the processes, which might occur during investigation on an electrode-material system, may be unavailable, premature, or perhaps too complicated to warrant its initial use. One then tries to show that the experimental impedance data $Z^e$ ($\omega$) may be well approximated by the impedance $Z^c$ ($\omega$) of an equivalent circuit made up of ideal resistors, capacitors, perhaps inductances, and possible various distributed circuit elements. In such a circuit, a resistance represents a conductive path, and a given resistor in the circuit might account for bulk conductivity of the material or even the chemical step associated with an electrode reaction. Similarly, capacitances and inductances could be generally associated with space charge polarization regions and with specific adsorption and electrocrystalisation processes at electrode. The physical interpretation of distributed elements in an equivalent circuit is somewhat more elusive. They are, however, essential in understanding and interpreting most impedance spectra. There are two types of distributions with which we need to be concerned. They both are related, but in different ways, to the finite spatial extension of any real system. The first type is associated directly with nonlocal processes, such as diffusion, which can occur even in completely homogeneous material for which the physical properties, such as charge mobilities, are the same everywhere. The other type, exemplified by constant-phase element (CPE), arises because microscopic material properties are themselves often distributed [27].

Basic model for description of dielectric properties of oxide films and bulk oxides is equivalent circuit -(R/C)- which consists of parallel connected resistance (R) and capacitance (C). Impedance of this circuit is:

$$Z^*_{RC} = \frac{R}{1 + j\omega RC} \tag{1}$$

The second important equivalent circuit is -(R/CPE)- which consists of parallel connected resistance $R$ and constant-phase element (CPE):

$$Z^*_{RCPE} = \frac{R}{1 + (j\omega RC)^n} \tag{2}$$

where $Z^*_{RC}$ and $Z^*_{RCPE}$ is complex impedance [Ω] of equivalent circuit -(R/C)- and equivalent circuit -(R/CPE)-, respectively, $R$ is resistance [Ω], $C$ is capacitance [F], $j = \sqrt{-1}$ is imaginary number, $\omega$ is angular frequency [rad·s$^{-1}$] ($\omega = 2\pi f$, where $f$ is frequency [Hz]), $n$ is empirical parameter related to non-ideal behaviour.

When

$$\tau = RC \tag{3}$$

where $\tau$ is relaxation time [s],
and

$$\tau = \frac{1}{2\pi f_{\max}} \tag{4}$$

the Equation 1 and Equation 2 can be expressed as:

$$Z^*_{RC} = \frac{R}{1 + jf/f_{\max}} \tag{5}$$

$$Z^*_{RCPE} = \frac{R}{1 + (jf/f_{\max})^n} \tag{6}$$

where the $f_{max}$ stands for the characteristic frequency of circuit.

In the case that there are more relaxation processes are in the examined material, combinations of several substitute circuits are used for the analysis of measured impedance spectra. Their connection can be parallel or serial. More advantageous is the usage of models that consist of serial connected resistance and -(R/C)- or -(R/

CPE)- elements, because they enable us to assign the particular relaxation processes to particular element. Subsequently, it is possible to identify at which of them relative humidity values are connected with particular breakthrough states of air humidity adsorption on the layer surface, caused by physical adsorption [27-30].

In our thesis, we study dependence of the number of equal circuits, which correspond with particular relaxation processes, on the relative humidity values for examined compounds of $SiO_2$-$TiO_2$-$Al_2O_3$ films.

## EXPERIMENTAL

### Preparation of sols

For synthesis of sols, titanium(IV) isopropoxide (98 %, $Ti(iPr)_4$), tetraethyl orthosilicate (98 %, TEOS), aluminum acetylacetonate (p.a., $Al(AcAc)_3$), isopropyl alcohol (p.a., IPA), acetylacetone (p.a., AcAc), nitric acid (65 %, $HNO_3$) and distilled water ($H_2O$) were used. Process of sol preparation is shown in the Figure 1. For the preparation of $SiO_2$–$TiO_2$–$Al_2O_3$ sols (procedure C), $SiO_2$-$Al_2O_3$ sol (procedure A) and $TiO_2$-$Al_2O_3$ sol (procedure B) were prepared at first. For the $SiO_2$–$Al_2O_3$ sol the molar ratios $HNO_3$:$SiO_2$ = 1 and $H_2O$:$SiO_2$ = 2 were used. For the $TiO_2$–$Al_2O_3$ sol the molar ratios AcAc:$TiO_2$ = = 0.6, $HNO_3$:$TiO_2$ = 0.5 and $H_2O$:$TiO_2$ = 1 were used. Table 1 shows the molar compositions of prepared sols, expressed as molar ratio, as well as assumed final molar ratio of $SiO_2$:$TiO_2$:$Al_2O_3$ in prepared films.

The $SiO_2$–$Al_2O_3$ sol was prepared by following procedure. Calculated amount of IPA was divided to two same parts. The solution of $HNO_3$ and water was added to the first part of IPA by dropwise during mixing and subsequently $Al(AcAc)_3$ was added. The solution was mixed until $Al(AcAc)_3$ was completely dissolved. The TEOS was added to the second part of IPA by dropwise during mixing. The first part of solution was added to the second part by dropwise during mixing and homogeneous $SiO_2$–$Al_2O_3$ sol was mixed for 15 minutes.

The $TiO_2$–$Al_2O_3$ sol was prepared by the same procedure as $SiO_2$–$Al_2O_3$ sol but the AcAc and $Ti(iPr)_4$ were added to the second part of IPA. After aging of both sols for 1 hour at room temperature, the $TiO_2$–$Al_2O_3$ sol was added to $SiO_2$–$Al_2O_3$ sol by dropwise and mixed for 15 minutes.

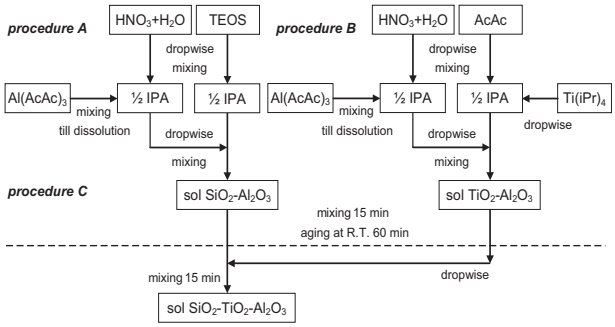


Figure 1. Procedure of sols preparation.

### Preparation of films

The films were deposited on the golden interdigital comb-like electrodes on $Al_2O_3$ substrate by dip-coating technique. Before the application, electrodes were cleaned in ammonia solution with hydrogen peroxide (1:3). Subsequently they were washed with distilled water, sonificated for 10 minutes and washed by isopropyl alcohol. Electrodes were coated by sol at rate of 90 mm·min$^{-1}$ and dried at 80°C for 15 minutes. Then, they were annealed at 400°C for 50 minutes at heating rate of 10°C·min$^{-1}$. After the heating process the electrodes were left in oven until the temperature decreased to 250°C. Subsequently, they were taken out from oven and stored to environment with relative humidity of 52.9 % where they were cooled freely to room temperature. The films were left in this environment for 24 hours.

### Characterization of films

Films on interdigital electrodes were investigated with atomic force microscope NT-206 (Co. Micro test Machines Belarus) in contact mode in the air using cantilever of MikroMasch CSC21/AlBS with spring force constant 2 N·m$^{-1}$.

Impedance spectra were measured at room temperature and relative humidities (RH) 0.13 %, 11.3 %, 23.1 %, 33.1 %, 43.1 %, 52.9 %, 59.1 %, 69.9 %, 75.5 %, 85.1 %, and 97.6 % in frequency interval from 1 kHz to 1 MHz, at voltage $U$ = 1.0 V by RCL Meter PM6306 Fluke machine. Particular relative humidities were obtained in closed PE containers above saturated solution of salts (Table 2), except the RH 0.13 % which was obtained above the silica.

Table 1. Molar composition of prepared sols and molar ratio of $SiO_2$:$TiO_2$:$Al_2O_3$ in prepared films.

| Sample | Component in sol (molar ratio) | | | | | | | $SiO_2$ : $TiO_2$ : $Al_2O_3$ in film (molar ratio) |
|---|---|---|---|---|---|---|---|---|
| | TEOS | $Ti(iPr)_4$ | $Al(AcAc)_3$ | AcAc | $HNO_3$ | $H_2O$ | IPA | |
| S0T1A | 0 | 0.0475 | 0.005 | 0.0435 | 0.0238 | 0.0475 | 0.835 | 0 : 0.95 : 0.05 |
| S1T2A | 0.0159 | 0.0317 | 0.005 | 0.0340 | 0.0317 | 0.0634 | 0.821 | 0.317 : 0.633 : 0.05 |
| S1T1A | 0.0238 | 0.0238 | 0.005 | 0.0293 | 0.0356 | 0.0713 | 0.814 | 0.475 : 0.475 : 0.05 |
| S2T1A | 0.0317 | 0.0159 | 0.005 | 0.0245 | 0.0396 | 0.0792 | 0.807 | 0.633 : 0.317 : 0.05 |
| S1T0A | 0.0475 | 0 | 0.005 | 0.0150 | 0.0475 | 0.0950 | 0.793 | 0.95 : 0 : 0.05 |

Table 2. Data on relative humidities [31].

| Saturated solution | RH [%] at 20°C |
|---|---|
| Silica gel | 0.13 |
| LiCl | 11.3 |
| $CH_3COOK$ | 23.1 |
| $MgCl_2$ | 33.1 |
| $K_2CO_3$ | 43.2 |
| $MgNO_3$ | 52.9 |
| NaBr | 59.1 |
| KI | 69.9 |
| NaCl | 75.5 |
| KCl | 85.1 |
| $K_2SO_4$ | 97.6 |

Measured dependences of complex impedance on frequency were processed by complex nonlinear least squares method [27, 29]. MATLAB® software was used for calculations. Serial connection with different counts of -(R/C)-, -(R/CPE)- and -R- equivalent circuits was used (Figure 2).

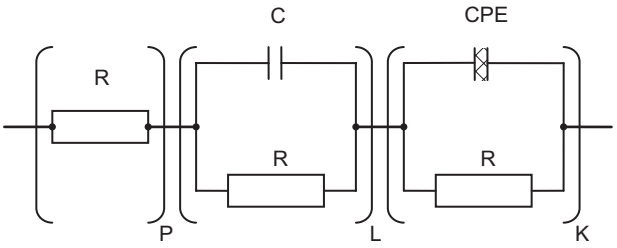


Figure 2. Serial connection with P, L, K counts of -R- , -(R/C)-, -(R/CPE)- equivalent circuits in model.

The impedance of model was calculated:

$$Z^*(f) = \sum_{p=0}^{P} R_p + \sum_{l=0}^{L} \frac{R_l^{RC}}{1 + jf \Big/ \left(f_{\max}^{RC}\right)_l} + R_k + \sum_{k=0}^{K} \frac{R_k^{RCPE}}{1 + \left(jf \Big/ \left(f_{\max}^{RCPE}\right)_l\right)^n} \tag{7}$$

where $P$, $L$, $K$ is count of -R-, -(R/C)-, -(R/CPE)- equivalent circuits in model. Then the last squares problem can be formulated:

$$S = \sum_{i=1}^{m} \left\{ w_i' \left[ \left(Z_i'\right)^e - \left(Z_i'\right)^c \right]^2 + w_i'' \left[ \left(Z_i''\right)^e - \left(Z_i''\right)^c \right]^2 \right\} = \min \tag{8}$$

where $(Z'_i)^e$, $(Z'_i)^c$ stand for experimental and calculated real part of complex impedance, $(Z''_i)^e$, $(Z''_i)^c$ represent experimental and calculated imaginary part of complex impedance, $w''_i$, $w'_i$ are statistical weights of real and imaginary part of complex impedance and $m$ is number of points.

Precision and accuracy of the model was verified on the basis of sum of squares of deviations and correlation coefficient. The differences between the calculated and experimental values were less than ten percent.

## RESULTS AND DISCUSSION

Measured impedance spectra were analysed by using the substitute circuits. The optimal model was determined by testing different models. The model with minimal value of objective function $S$ was chosen.

In the Figure 3, there are comparisons of measured and calculated impedance spectra for the composition S2T1A at RH = 11.3 % (Figure 3a); suitable model was -R-(R/C)-(R/CPE)- and for the composition S0T1A at RH = 97.6 % (Figure 3b); suitable model was -R-($R_1$/$C_1$)-($R_2$/$C_2$)-(R/CPE)-. Within the file of measured spectra, we found out that model -R-(R/C)-(R/CPE)-, further marked as 3, was suitable for low RH values. At higher humidity values, the best results were observed with the

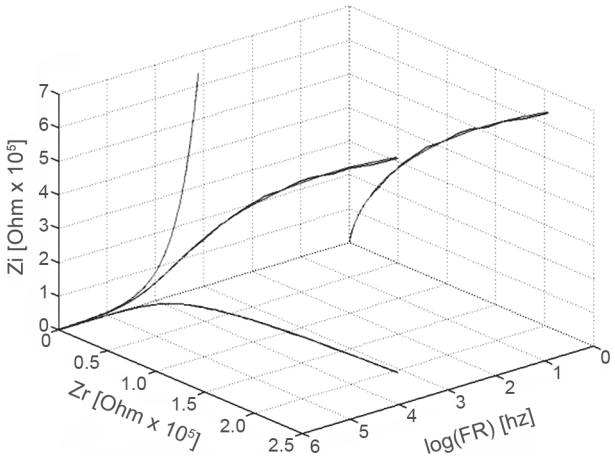


a) S2T1A at RH = 11.3 %

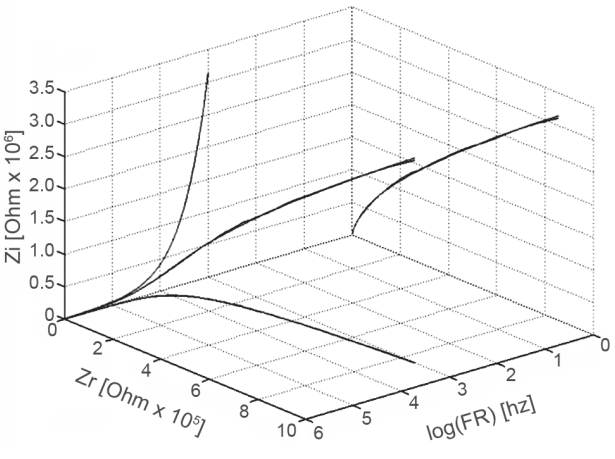


b) S0T1A at RH = 97.6 %

Figure 3. Comparison of measured and calculated impedance spectra for: a) the composition S2T1A at RH = 11.3 %; suitable model was -R-(R/C)-(R/CPE)-, b) the composition S0T1A at RH = 97.6 %; suitable model was -R-($R_1$/$C_1$)-($R_2$/$C_2$)-(R/CPE)-.

model -R-($R_1$/$C_1$)-($R_2$/$C_2$)-(R/CPE)-, further marked as 4. In some cases, at the highest RH values, it was necessary to apply more complicated models, further marked as 5. At RH = 0.13 %, some of the prepared samples showed impedance values beyond the apparatus range, further marked as 0.

3D AFM images of electrode surface without film and surfaces of films deposited on interdigital electrode are shown in Figure 4. AFM images show that application of $SiO_2$–$TiO_2$–$Al_2O_3$ films on interdigital electrodes does not cause significant changes of surface morphology. No observable pores, cracks and sharp rib edges are on the surface of films. The differences are in rms roughness of surface. The rms roughness for S1T0A film is the highest (105 nm) and for S1T1A film is the lowest (56 nm). Thickness of films coated on this substrate can be only estimated. On the basis of measurement the thickness of $SiO_2$–$TiO_2$–$Al_2O_3$ films coated on glass, we can assume that thickness of films on electrodes is in the range of 80 - 100 nm.

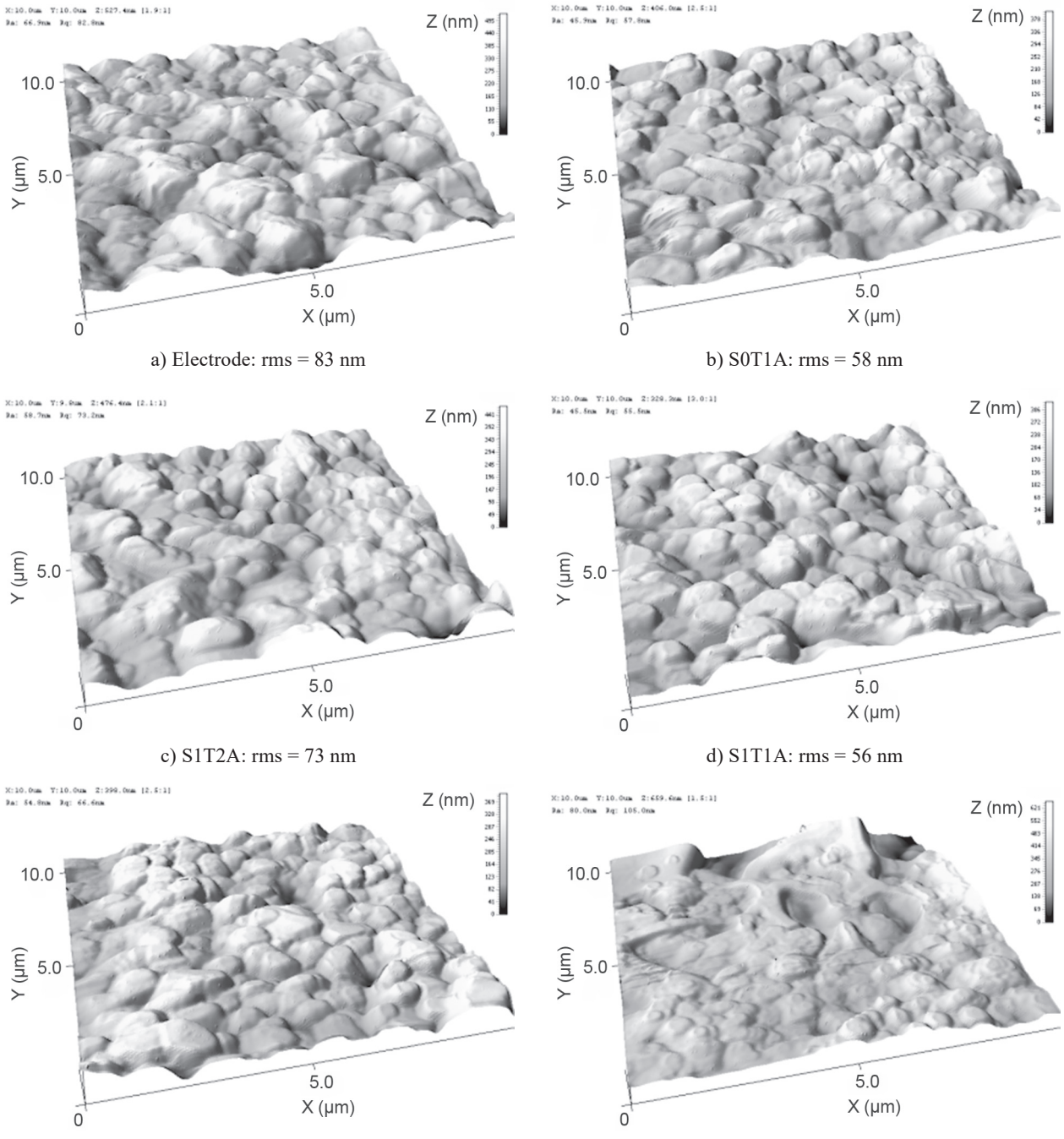


a) Electrode: rms = 83 nm

b) S0T1A: rms = 58 nm

c) S1T2A: rms = 73 nm

d) S1T1A: rms = 56 nm

e) S2T1A: rms = 67 nm

f) S1T0A: rms = 105 nm

Figure 4. 3D AFM images of electrode surface without film and surfaces of films deposited on interdigital electrode and their rms roughness.

According to results of AFM measurements and data in the Figure 5, measured dependence of the number of circuit elements on the composition (expressed as $SiO_2$ molar ratio) and on the air humidity values can be clarified in pursuance of these following assumptions.

There are three cognizable stages of process of physical adsorption of water on the materials surfaces, in our case on the $SiO_2$–$TiO_2$–$Al_2O_3$ films. In the first stage, at low RH values, adsorbed water creates islets which affect the dielectric properties of layer. The islets are created on surface and they will not become evident with individual relaxation process. The second stage is in connection with higher RH values. In this stage, coherent layer of adsorbed water is formed. Water molecules in this layer are relatively tightly bound with the layer surface by hydrogen bonds therefore their mobility is limited. The coherent layer of adsorbed water will become evident with individual relaxation process. In the third stage, at the high RH values, more layers of water molecules are adsorbed on the layer which was created in the second stage. Water molecules in these layers are bounded among them and therefore they have relatively high mobility. This leads to the creation of another polarization process. The adsorption of water on the film surface depends on concentration of –OH groups and surface roughness.

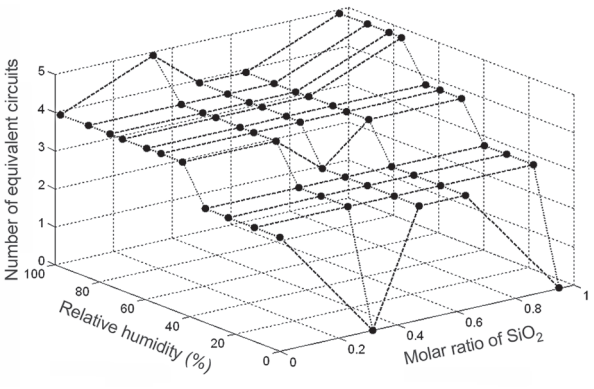


Figure 5. Dependence of the number of the elements on the molar ratio of $SiO_2$ and relative humidity.

For examined compositions S0T1A, S1T2A, S2T1A and S1T0A ($SiO_2$ molar ratio 0, 0.317, 0.633 and 0.95), the transition between the first and the second stage of water adsorption (creation of coherent water layer) occurs at the RH values from 33.1 % to 43.2 %. For the composition S1T1A ($SiO_2$ molar ratio 0.475), this transition occurs at the RH values from 43.2 % to 52.9 %. The transition between the second and the third stage of water adsorption onto the surface of film was observed for the composition S1T2A at the RH values from 85.1 % to 97.6 % and for the composition S1T0A at the RH values from 59.1 % to 69.9 %. The transition between individual stages of water adsorption is connected with rms roughness and concentration of –OH groups on film surface. The rms roughness (56 nm) is the lowest for S1T1A film where the transition between the first and the second stage of water adsorption is at the RH values from 43.2 % to 52.9 %. The rms roughness (73 nm) is the second highest for S1T2A film where the transition between the second and the third stage of water adsorption is at the RH values from 85.1 % to 97.6 %. The rms roughness (105 nm) is the highest for S1T0A film where the transition between the second and the third stage of water adsorption is at the RH values from 59.1 % to 69.9 %. The transition to the third stage of water adsorption at relatively low values of RH is due to higher concentration of –OH groups on surface of this film. In comparison to other films, the relatively high concentration of –OH groups is caused by composition of S1T0A film which is $SiO_2$–$Al_2O_3$ film actually [6, 7, 12].

## CONCLUSION

Using the impedance spectroscopy, particular stages of physical adsorption of water and the transitions between them were identified for the examined compositions of $SiO_2$–$TiO_2$–$Al_2O_3$ films, expressed by $SiO_2$:$TiO_2$:$Al_2O_3$ ratio, in the range of following molar ratio: 0:0.95:0.05; 0.32:0.63:0.05; 0.475:0.475:0.05; 0.63:0.32:0.05; 0.95:0:0.05. In relation to S0T1A, S1T2A, S2T1A and S1T0A compositions ($SiO_2$ molar ratio 0, 0.317, 0.633 and 0.95), there was observed the transition between the second and the third stage, and the creation of compact water layer on surface occurs at the RH values from 33.1 % to 43.2 %. This transition is between RH values 43.2 % and 52.9 % for the S1T1A ($SiO_2$ molar ratio 0.475). Transition between the second and the third stage of water adsorption was observed for the S1T2A composition at the RH values from 85.1 % to 97.6 % and for the S1T0A composition at the RH values from 59.1 % to 69.9 %. The significant difference in the course of physical adsorption onto the S1T0A film ($SiO_2$:$TiO_2$:$Al_2O_3$ molar ratio 0.95:0:0.05) is clarified by rms roughness and higher concentration of –OH groups on the surface.

### Acknowledgement

*This work was supported by the Grant Agency of Slovak Republic – Grant No. 1/0559/11 and Grant No. 1/0006/12.*

## REFERENCES

1. Travesa E.: Sensors and Actuators B *23*, 135 (1995).
2. Korotcekov G.: Mat. Sci. Eng. B *139*, 1 (2007).
3. Atkins P.W.: *Physical Chemistry*, University Press, Oxford, 1998.

4. Scukin E.D., Percov A.V., Amelinova E.A.: *Koloidní chemie*, Academia, Praha, 1990.
5. Chou K.S., Lee T.K., Liu F.J.: Sensors and Actuators B *56*, 106 (1999).
6. Zhuralev L.T. in: *Colloidal Silica Fundamentals and Applications*, p. 261-266, Eds. H.E. Berga, W.O. Roberts, CRC Press Taylor & Francis Group, New York, 2006.
7. Casacarini de Torre L.E., Bottani E.J. in: *Colloidal Silica Fundamentals and Applications*, p. 311-359, Eds. H.E. Berga, W.O. Roberts, CRC Press Taylor & Francis Group, New York, 2006.
8. Agmon N.: Chem. Phys. Let. *244*, 456 (1995).
9. Cukierman S.: Biochim. Biophys. Acta *1757*, 876 (2006).
10. Chen Z., Lu Ch.: Sensor Letters *3*, 274 (2005).
11. Faia P.M., Ferreira A.J., Furtado C.S.: Sensors and Actuators B *140*, 128 (2009).
12. Brinker C.J., Scherer G.W.: *Sol-Gel Science : The Physics and Chemistry of Sol-Gel Processing*, Academic Press, Boston, 1990.
13. Plško A., Exnar P.: Silikáty *1*, 69 (1989).
14. Schmidt H.: J. Sol-Gel Sci. Technol. *40*, 115 (2006).
15. Carmona N., Herrero E., Llopis J., Villegas M.A.: Sensors and Actuators B *126*, 455 (2007).
16. Vaivars G., Pitkevičs J., Lusis A.: Sensors and Actuators B *13-14*, 111 (1993).
17. Yuk J., Troczynski T.: Sensors and Actuators B *94*, 290 (2003).
18. Mistry K.K., Saha D., Sengupta K.: Sensors and Actuators B *106*, 258 (2005).
19. Montesperelli G., Pumo A., Traversa E., Gusmano G., Bearzotti A., Montenero A., Gnappi G.: Sensors and Actuators B *24-25*, 705 (1995).
20. Plško A., Papučová I., Faturíková K., Pagáčová J., Šulcová J. in: Preparation of Ceramic Materials: Proceedings IXth International Conference, p. 44-48, Technical Universiy, Košice, 2011.
21. Faturíková K., Plško A., Pagáčová J., Papučová I., Šulcová J. in: Preparation of Ceramic Materials: Proceedings IXth International Conference, p. 30-34, Technical Universiy, Košice, 2011.
22. Biju K.P., Jain M.K.: Sensors and Actuators B *128*, 407 (2008).
23. Ponce M.A., Parra R., Savu R., Joanni E., Bueno P.R., Cilense M., Varela J.A., Castro M.S.: Sensors and Actuators B *139*, 447 (2009).
24. Metikoš-Huković M., Omanović S., Jukić A.: Electrochim. Acta *45*, 977 (1999).
25. Endres H.-E., Drost S., Hutted F.: Sensors and Actuators B *22*, 7 (1994).
26. Abdelghani A., Cherif K., Jaffrezic-Renault N., Matejec V.: Mater. Sci. Eng. C *26*, 542 (2006).
27. Barsoukov E., Macdonald J.R.: *Impedance Spectroscopy Theory, Experiment, and Applications*, Wiley, New Jersy, 2005.
28. Raju G.G.: *Dielectrics in Electric Fields*, Marcel Dekker AG, New York, 2003.
29. Macdonald J.R.: Solid State Ionics *176*, 1961 (2005).
30. Shoar Abouzari M.R., Berkemeier F., Schmitz G., Wilmer D.: Solid State Ionics *180*, 922 (2009).
31. ASTM E-104-02 (2007) Standard Practice for Maintaining Constant Relative Humidity by Means of Aqueous Solution, ASTM International, Pennsylvania, United States 5p.